

Unexpected fullerene dimerization *via* [5,6]-bond upon functionalization of C_s-C₇₀(CF₃)₈ by the Bingel reaction

N.S. Ovchinnikova, A.A. Goryunkov, P.A. Khavrel, N.M. Belov, M.G. Apenova, I.N. Ioffe, M.A. Yurovskaya, S.I. Troyanov, L.N. Sidorov and E. Kemnitz

in Dalton Transactions

Table of contents

- **Figures S1–S4.** Top and side projections of {C₇₀(CF₃)₈[C(CO₂Et)₂]_n}₂, n=0–2, according to X-Ray data S2–5
- **Figures S5, S6.** Cyclobutane and cyclopropane moieties of {C₇₀(CF₃)₈[C(CO₂Et)₂]}₂-I S6
- **Figure S7.** HPLC and MS MALDI data of oxidized sample of C₇₀(CF₃)₈[C(CO₂Et)₂]-I S7
- **Figures S8, S9.** ¹H and ¹⁹F NMR spectra of C₇₀(CF₃)₈[C(CO₂Et)₂]-I S8
- **Figures S10, S11.** ¹H and ¹⁹F NMR spectra of C₇₀(CF₃)₈[C(CO₂Et)₂]-I, CH₃ protons decoupled S9
- **Figures S12, S13.** ¹H and ¹⁹F NMR spectra of C₇₀(CF₃)₈[C(CO₂Et)₂]-II S10
- **Figures S14, S15.** ¹H and ¹⁹F NMR spectra of C₇₀(CF₃)₈[C(CO₂Et)₂]-II, CH₃ protons decoupled S11
- **Figures S16, S17.** ¹H and ¹⁹F NMR spectra of C₇₀(CF₃)₈[C(CO₂Et)₂]₂ S12
- **Figures S18, S19, S20.** 2D COSY ¹H NMR spectrum of C₇₀(CF₃)₈[C(CO₂Et)₂]₂ with magnified regions. S13–S15
- **Figures S21, S22.** UV/Vis spectra of C₇₀(CF₃)₈[C(CO₂Et)₂]_n, n=0–2, and C₇₀(CF₃)₈[C(CO₂Et)₂O-I] S16
- **Table S1.** Calculation details S17
- **Table S2.** Schlegel diagrams, relative energies (at the DFT, single point DFT and AM1 levels of theory) for the most stable isomers of C₇₀(CF₃)₈C(CO₂Et)₂ within the DFT energy gap of 40 kJ mol⁻¹. S18
- **Table S3.** Schlegel diagrams, relative energies (at the DFT, single point DFT and AM1 levels of theory) for the most stable anions C₇₀(CF₃)₈R⁻ (R=CBr(CO₂Et)₂ and H) within the DFT energy gap of 50 kJ mol⁻¹. S20
- **Table S4.** Schlegel diagrams, relative DFT energies and fragments of 3D projections of C₇₀(CF₃)₈[CBr(CO₂Et)₂]⁻ anionic intermediates S22
- **Table S5.** Schlegel diagrams, relative energies (at the DFT, single point DFT and AM1 levels of theory) for the most stable isomers of C₇₀(CF₃)₈[C(CO₂Et)₂]₂ within the DFT energy gap of 30 kJ mol⁻¹. S24

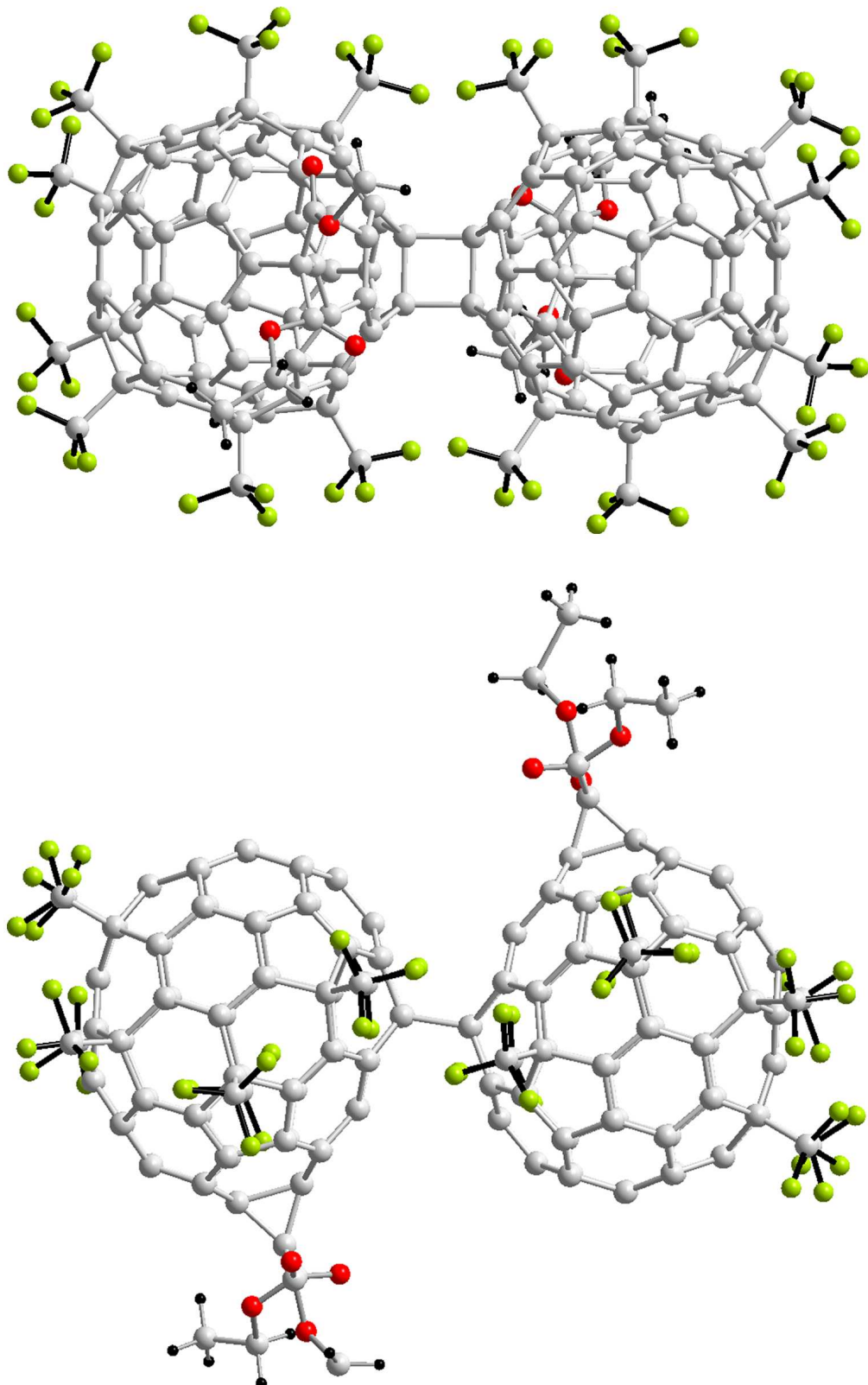


Figure S1. Top and side projections of $\{C_{70}(CF_3)_8[C(CO_2Et)_2]\}_2\text{-I}$.

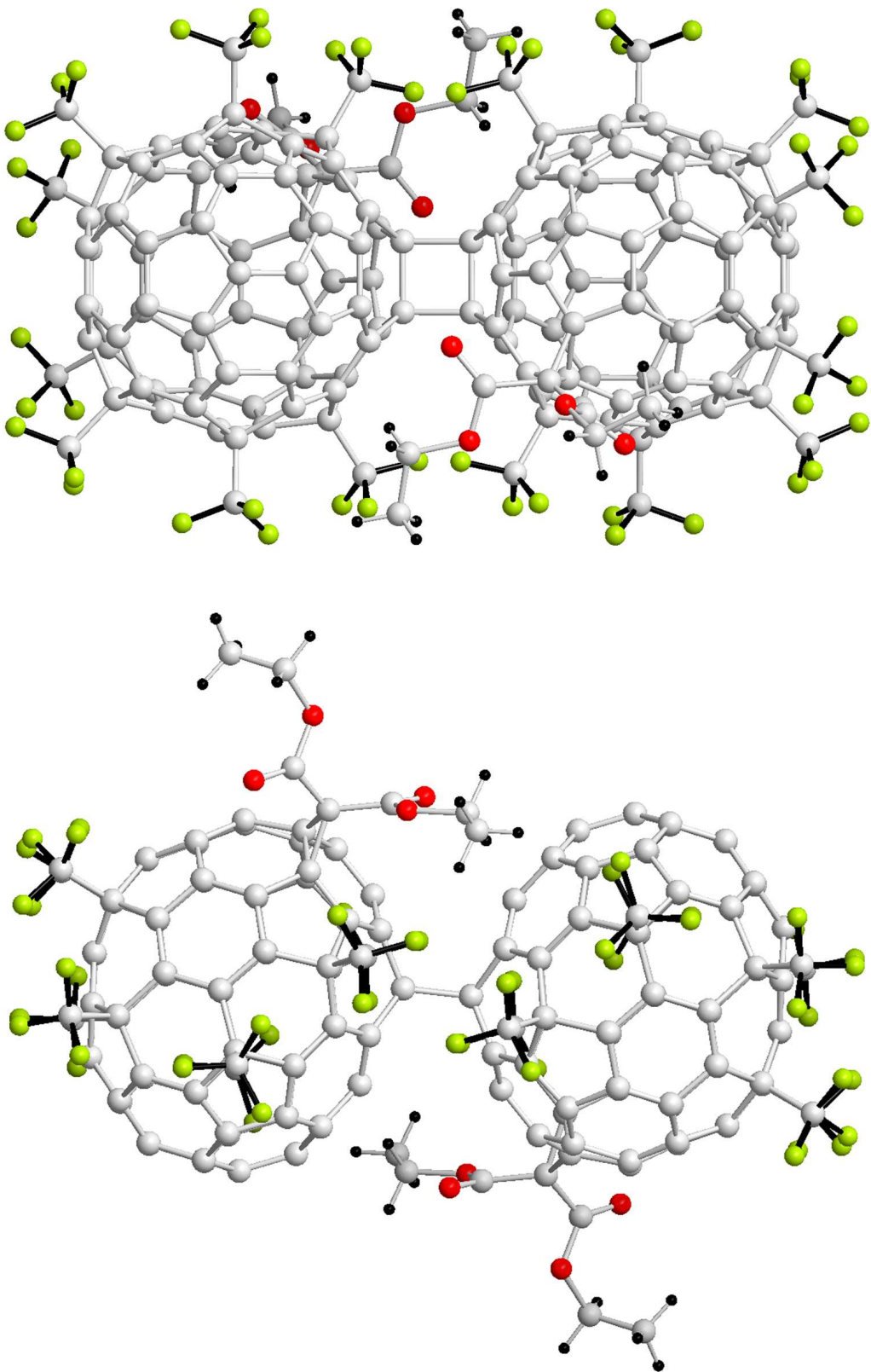


Figure S2. Top and side projections of $\{C_{70}(CF_3)_8[C(CO_2Et)_2]\}_2$ -II.

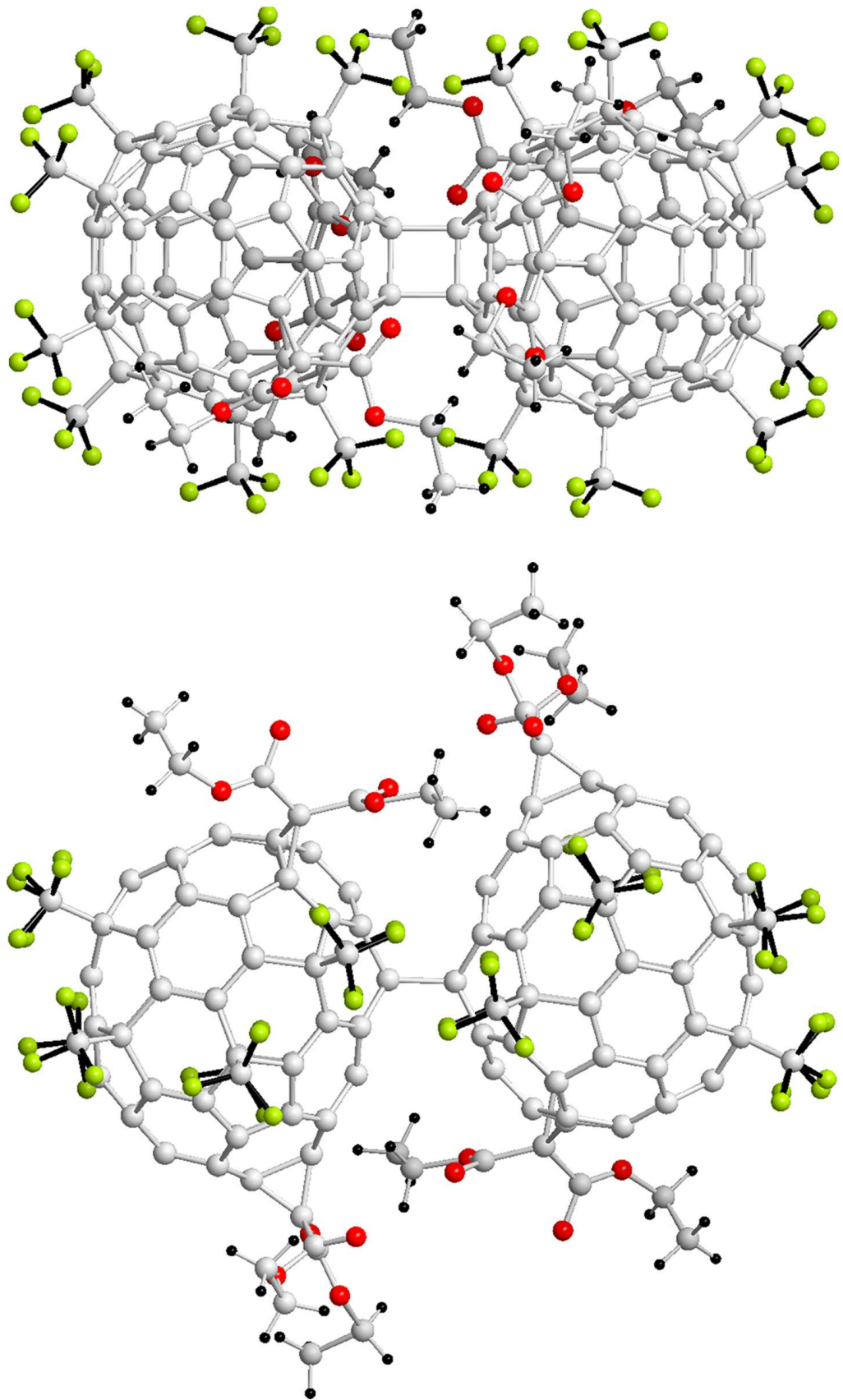


Figure S3. Top and side projections of $\{C_{70}(CF_3)_8[C(CO_2Et)_2]_2\}_2$.

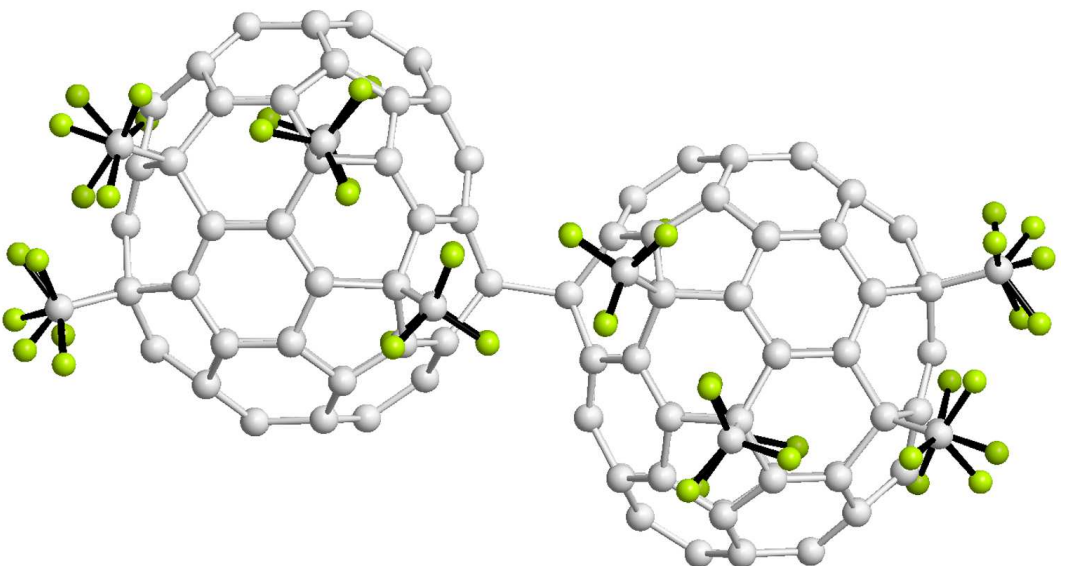
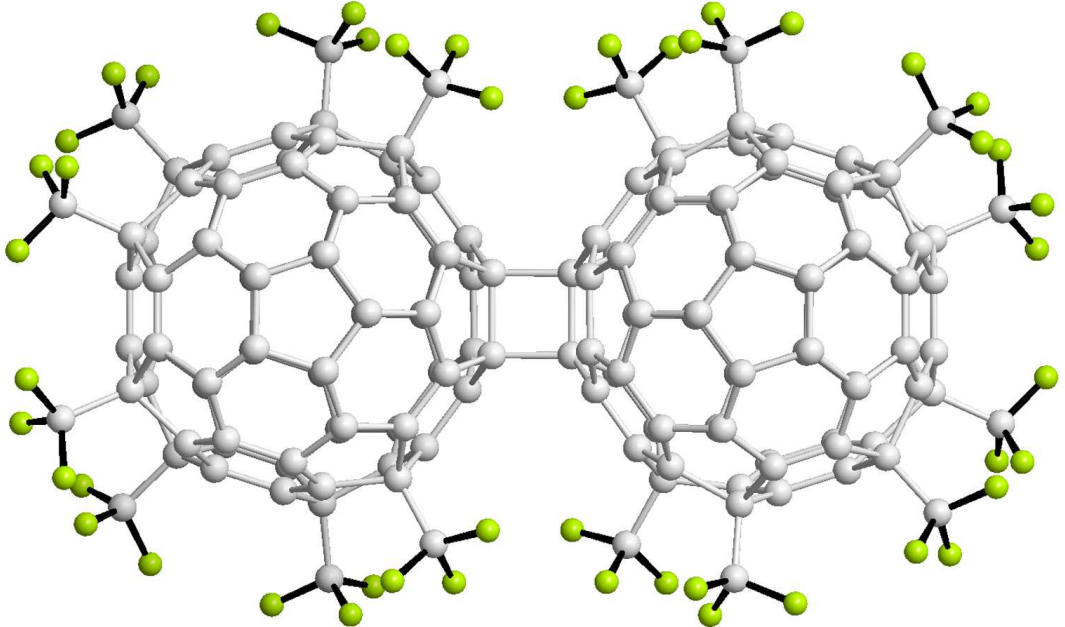


Figure S4. Top and side projections of $\{C_{70}(CF_3)_8\}_2$.

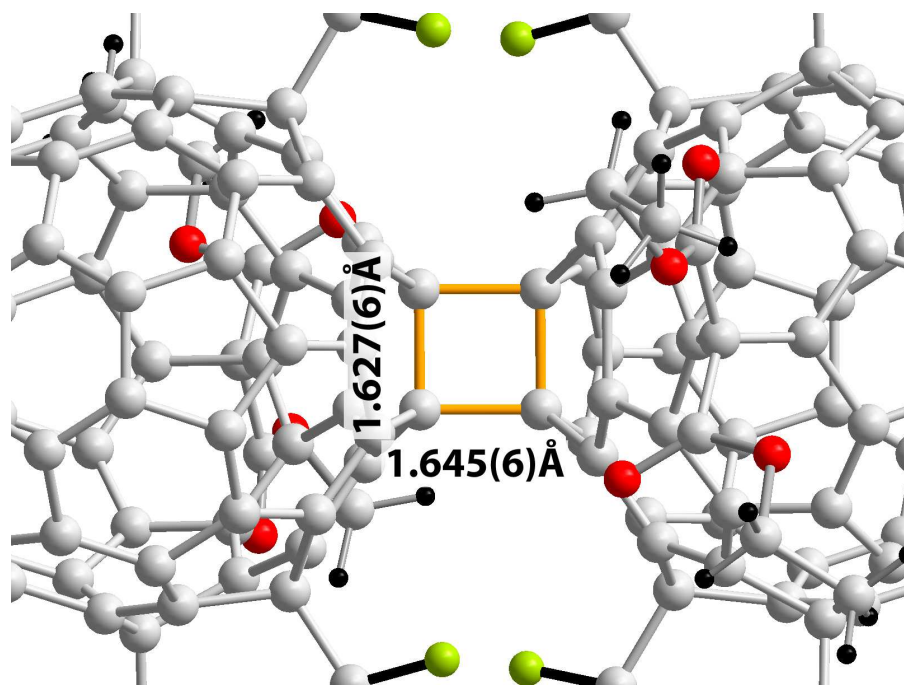


Figure S5. Cyclobutane connection of bispherical $\{C_{70}(CF_3)_8[C(CO_2Et)_2]\}_2\text{-I}$

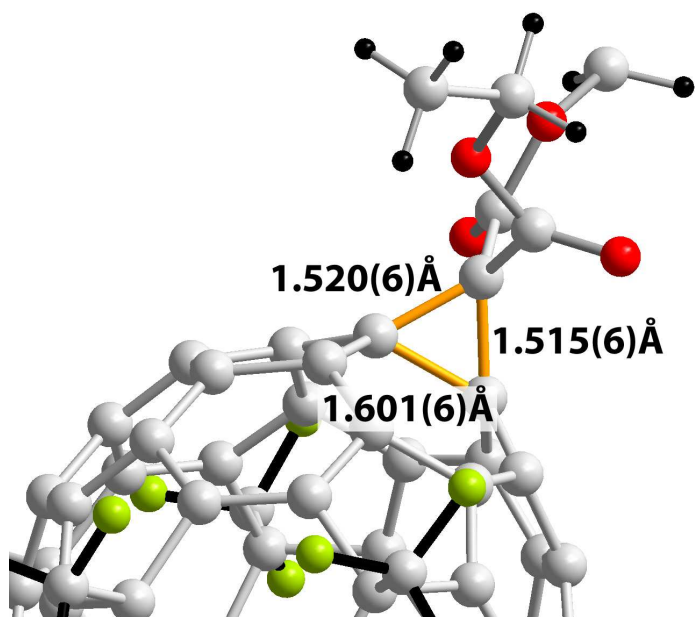


Figure S6. Cyclopropane moiety in the structure $\{C_{70}(CF_3)_8[C(CO_2Et)_2]\}_2\text{-I}$

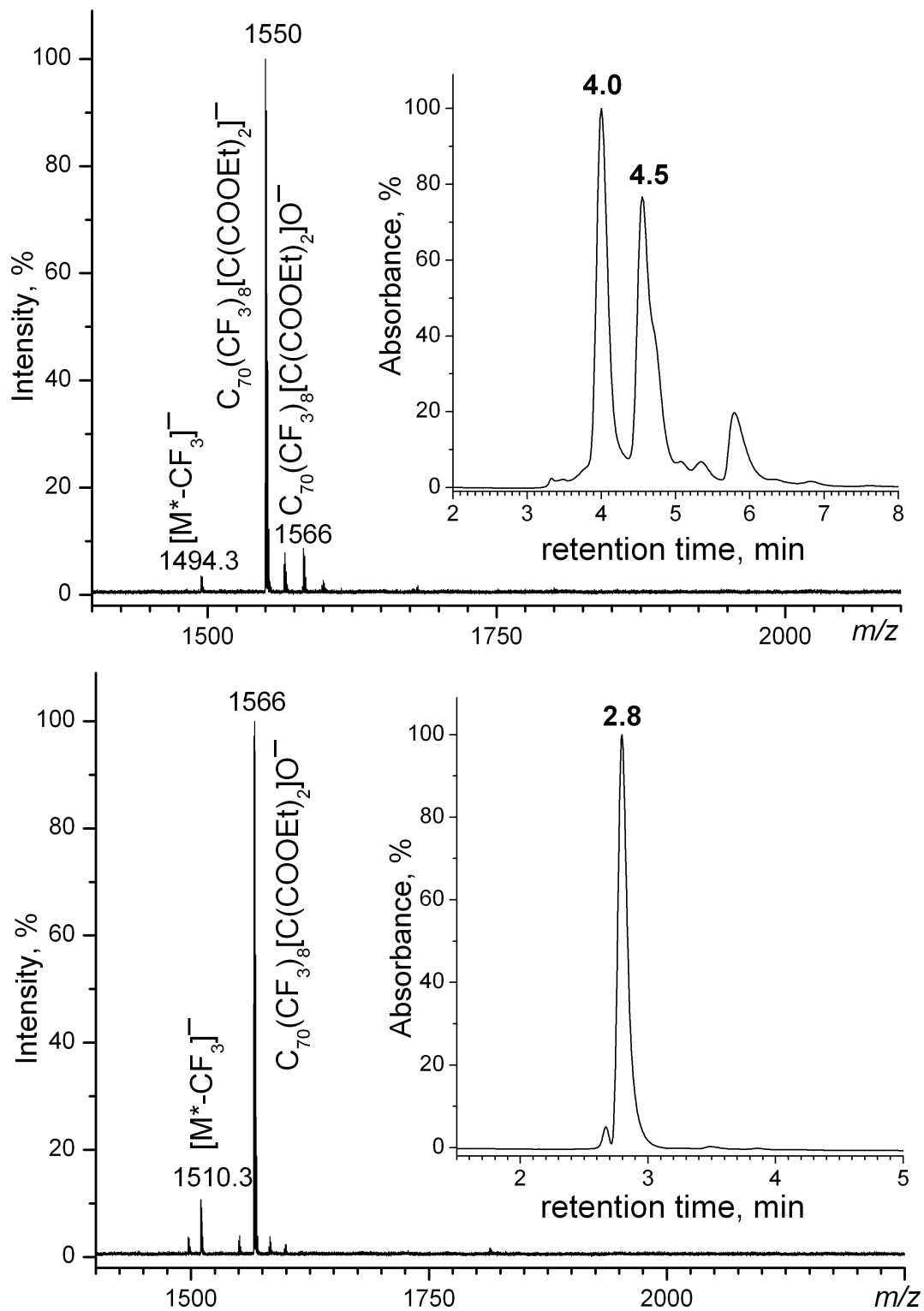


Figure S7. The negative ion MALDI mass spectrum and the HPLC trace (inset, *Cosmosil Buckyprep 10 I.D. mm × 25 cm, toluene, 4.6 mL·min⁻¹*) of fraction **p1** after NMR analysis (top). The negative ion MALDI mass spectrum and the HPLC trace (inset, *Cosmosil Buckyprep 4.6 I.D. mm × 25 cm, toluene, 2 mL·min⁻¹*) of fraction with retention time 4.0 min (bottom).

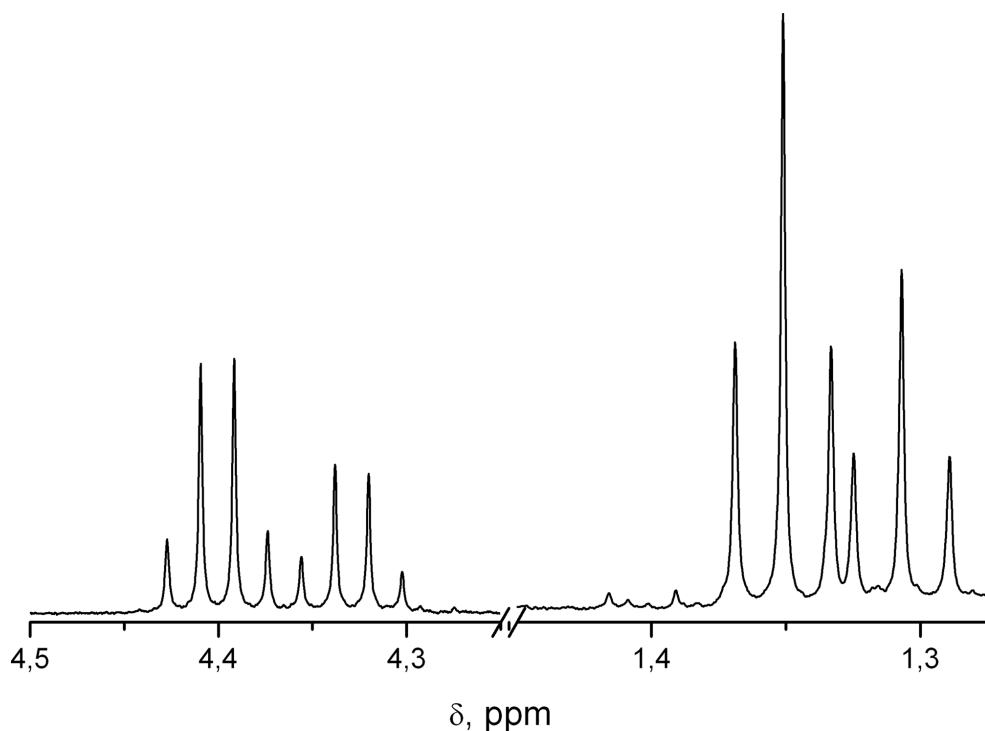


Figure S8. ^1H NMR spectrum of $\text{C}_{70}(\text{CF}_3)_8[\text{C}(\text{CO}_2\text{Et})_2]\text{-I}$

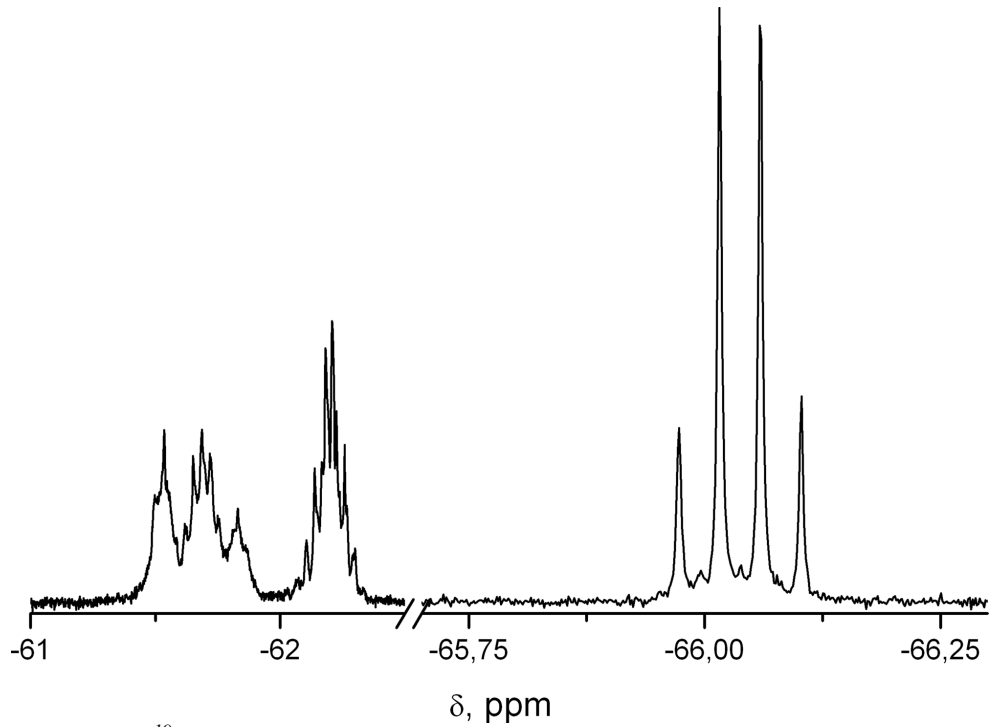


Figure S9. ^{19}F NMR spectrum of $\text{C}_{70}(\text{CF}_3)_8[\text{C}(\text{CO}_2\text{Et})_2]\text{-I}$

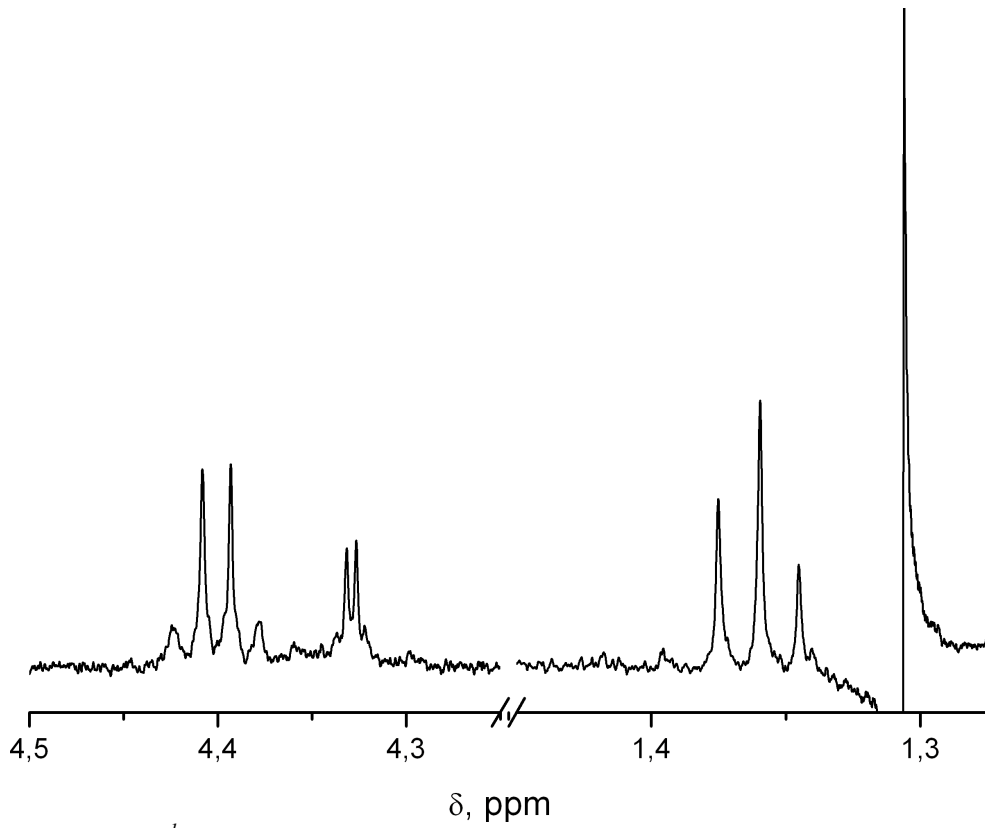


Figure S10. ^1H NMR spectrum of $\text{C}_{70}(\text{CF}_3)_8[\text{C}(\text{CO}_2\text{Et})_2]\text{-I}$, CH_3 protons ($\delta=1.31$ ppm) decoupled

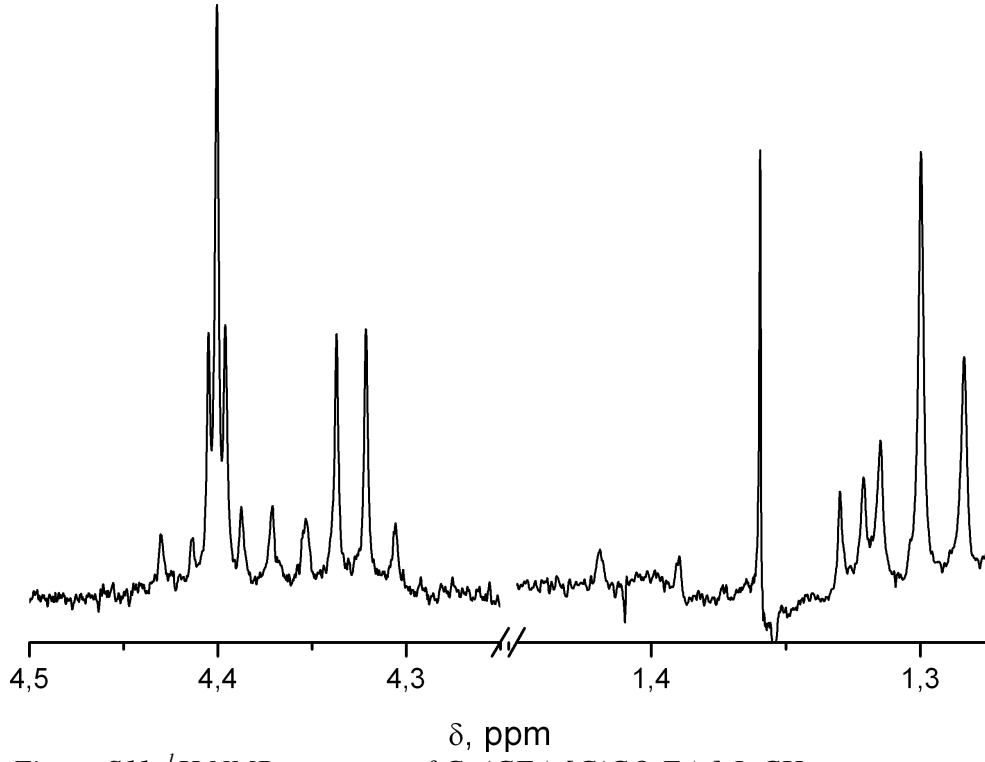


Figure S11. ^1H NMR spectrum of $\text{C}_{70}(\text{CF}_3)_8[\text{C}(\text{CO}_2\text{Et})_2]\text{-I}$, CH_3 protons ($\delta=1.36$ ppm) decoupled

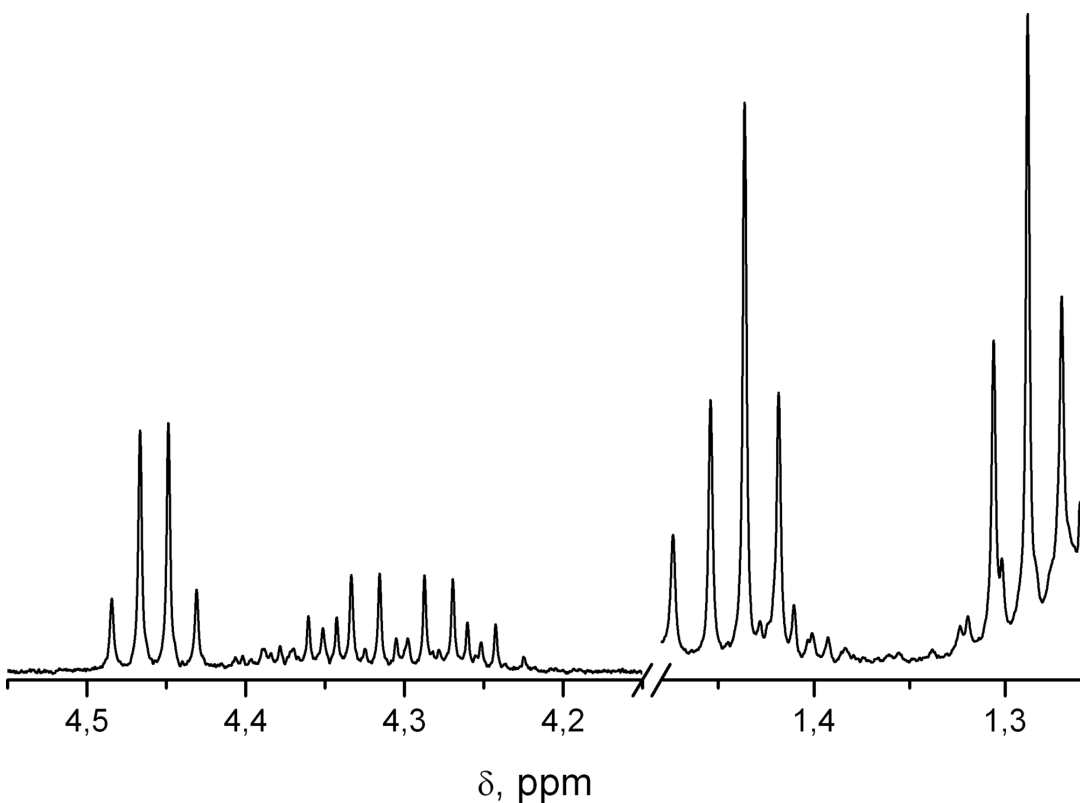


Figure S12. ^1H NMR spectrum of $\text{C}_{70}(\text{CF}_3)_8[\text{C}(\text{CO}_2\text{Et})_2]\text{-II}$

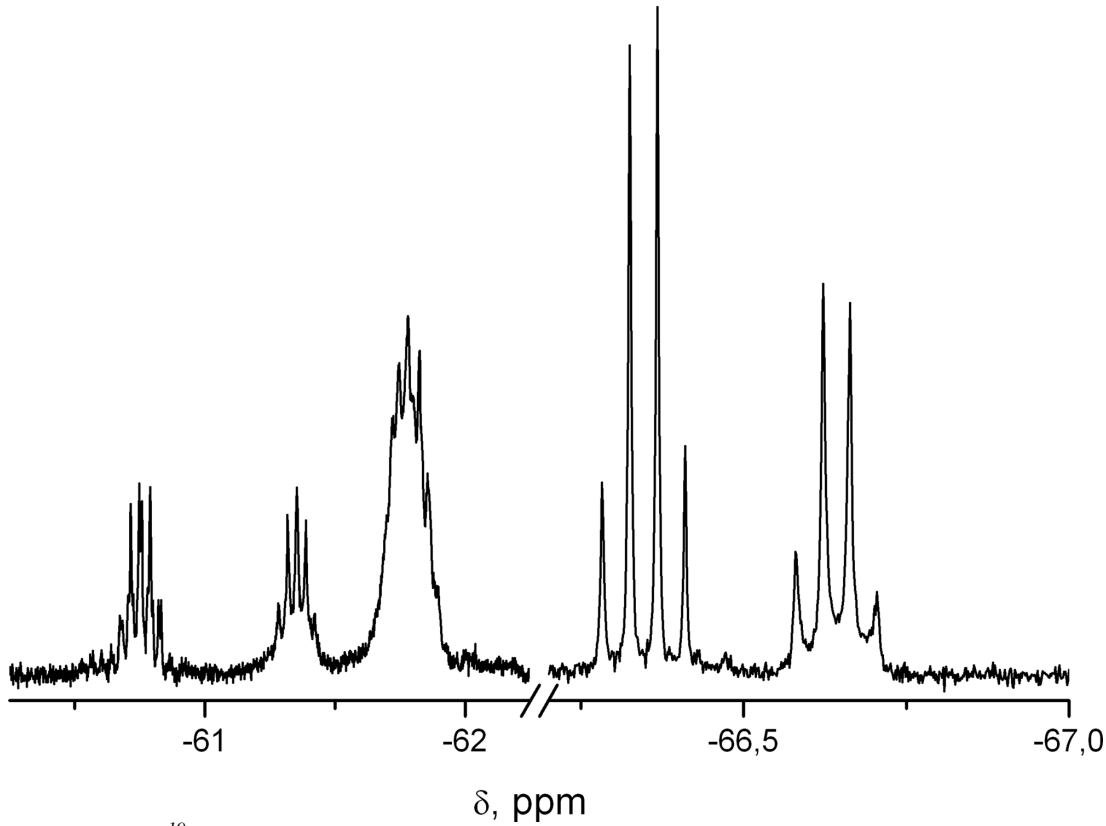


Figure S13. ^{19}F NMR spectrum of $\text{C}_{70}(\text{CF}_3)_8[\text{C}(\text{CO}_2\text{Et})_2]\text{-II}$

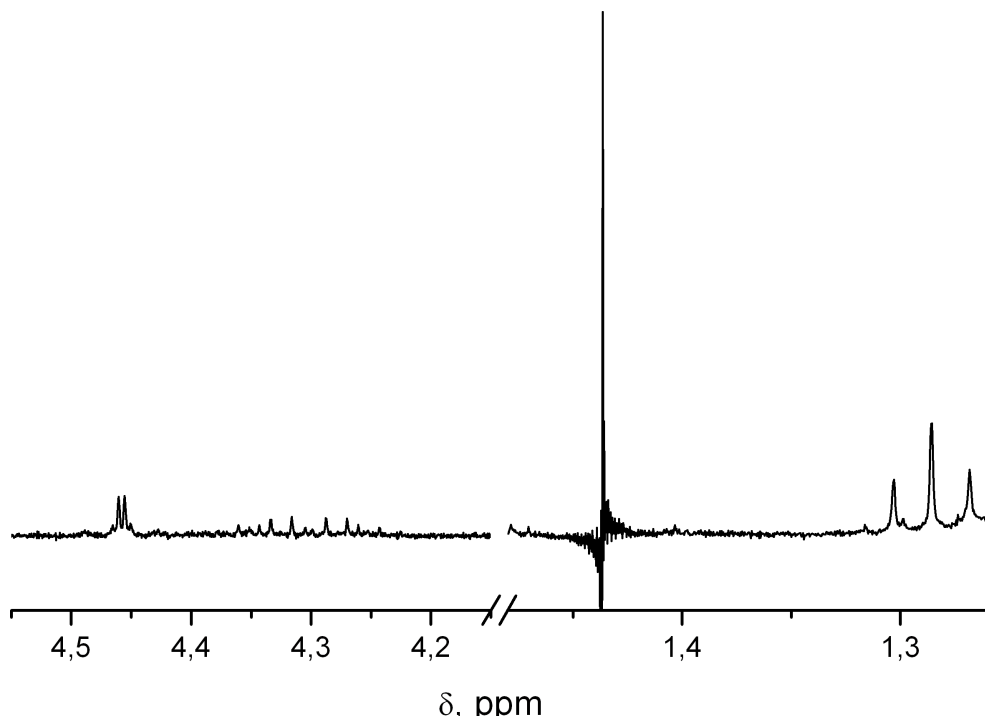


Figure S14. ^1H NMR spectrum of $\text{C}_{70}(\text{CF}_3)_8[\text{C}(\text{CO}_2\text{Et})_2]\text{-II}$, CH_3 protons ($\delta=1.44$ ppm) decoupled

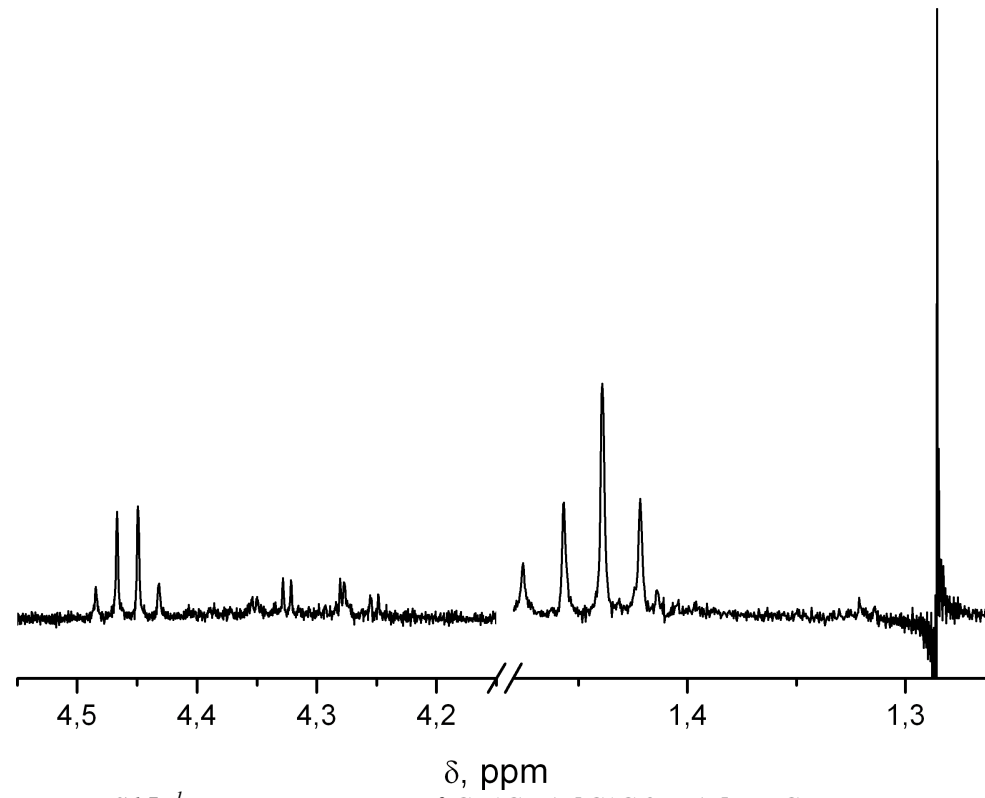


Figure S15. ^1H NMR spectrum of $\text{C}_{70}(\text{CF}_3)_8[\text{C}(\text{CO}_2\text{Et})_2]\text{-II}$, CH_3 protons ($\delta=1.29$ ppm) decoupled

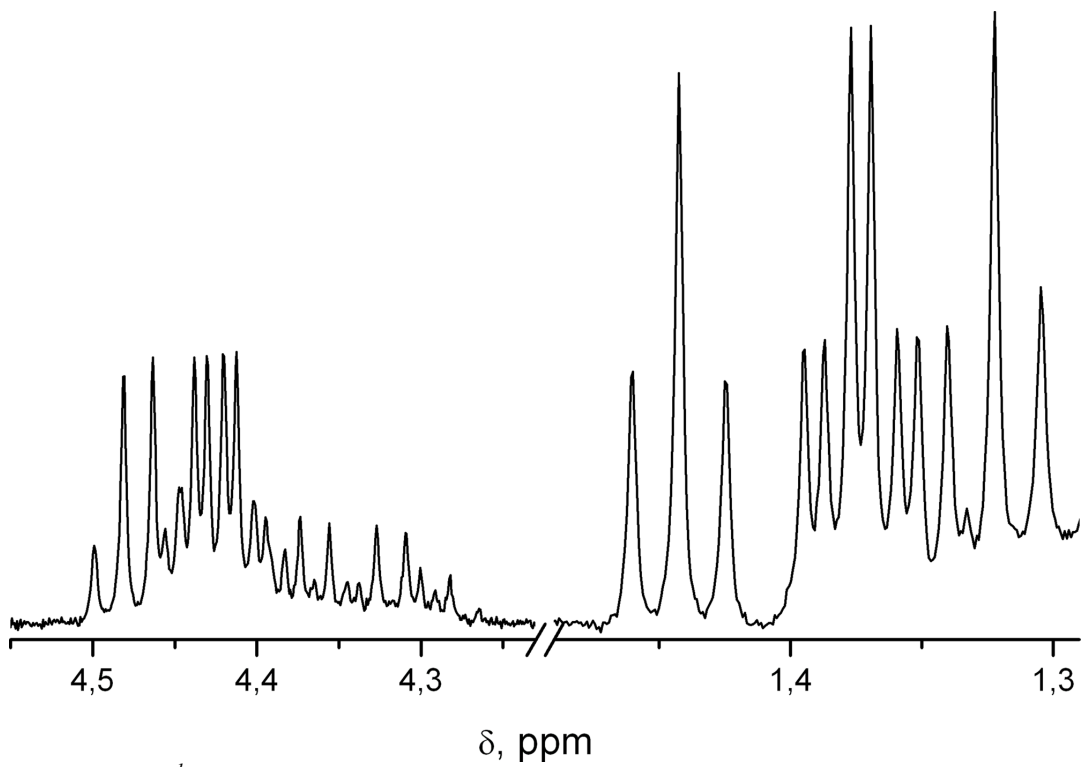


Figure S16. ^1H NMR spectrum of $\text{C}_{70}(\text{CF}_3)_8[\text{C}(\text{CO}_2\text{Et})_2]_2$

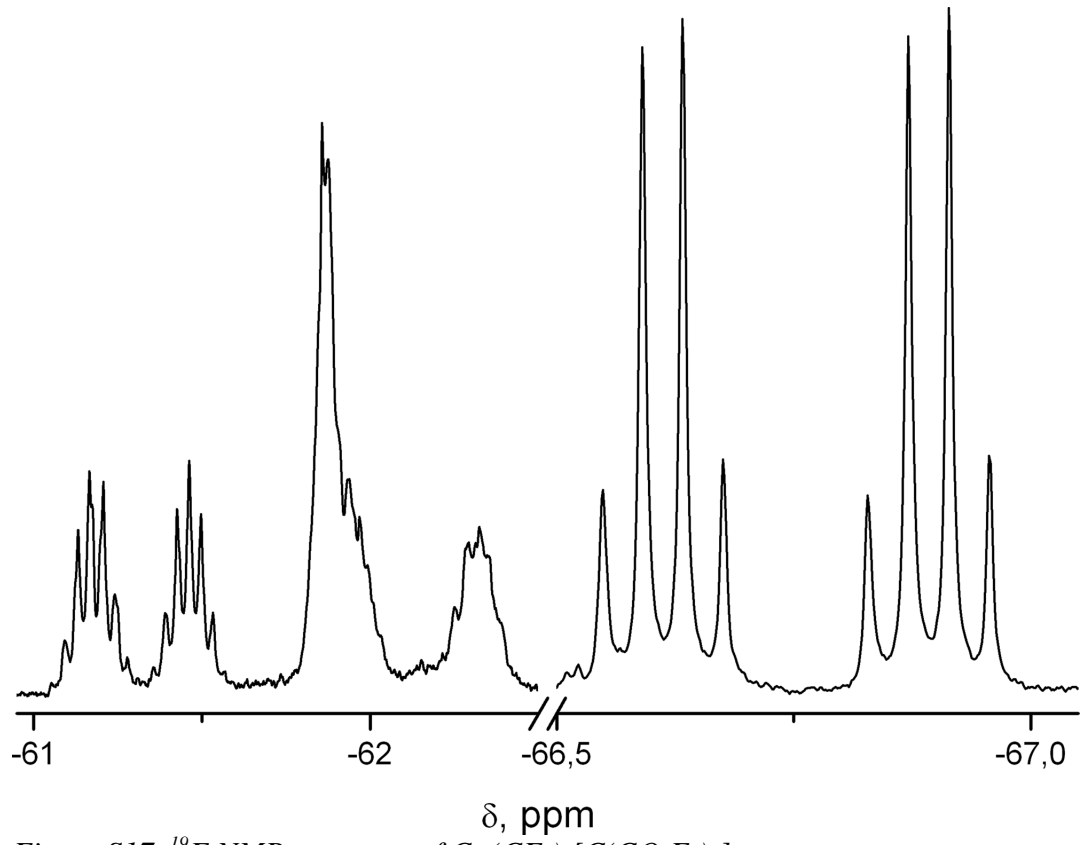


Figure S17. ^{19}F NMR spectrum of $\text{C}_{70}(\text{CF}_3)_8[\text{C}(\text{CO}_2\text{Et})_2]_2$

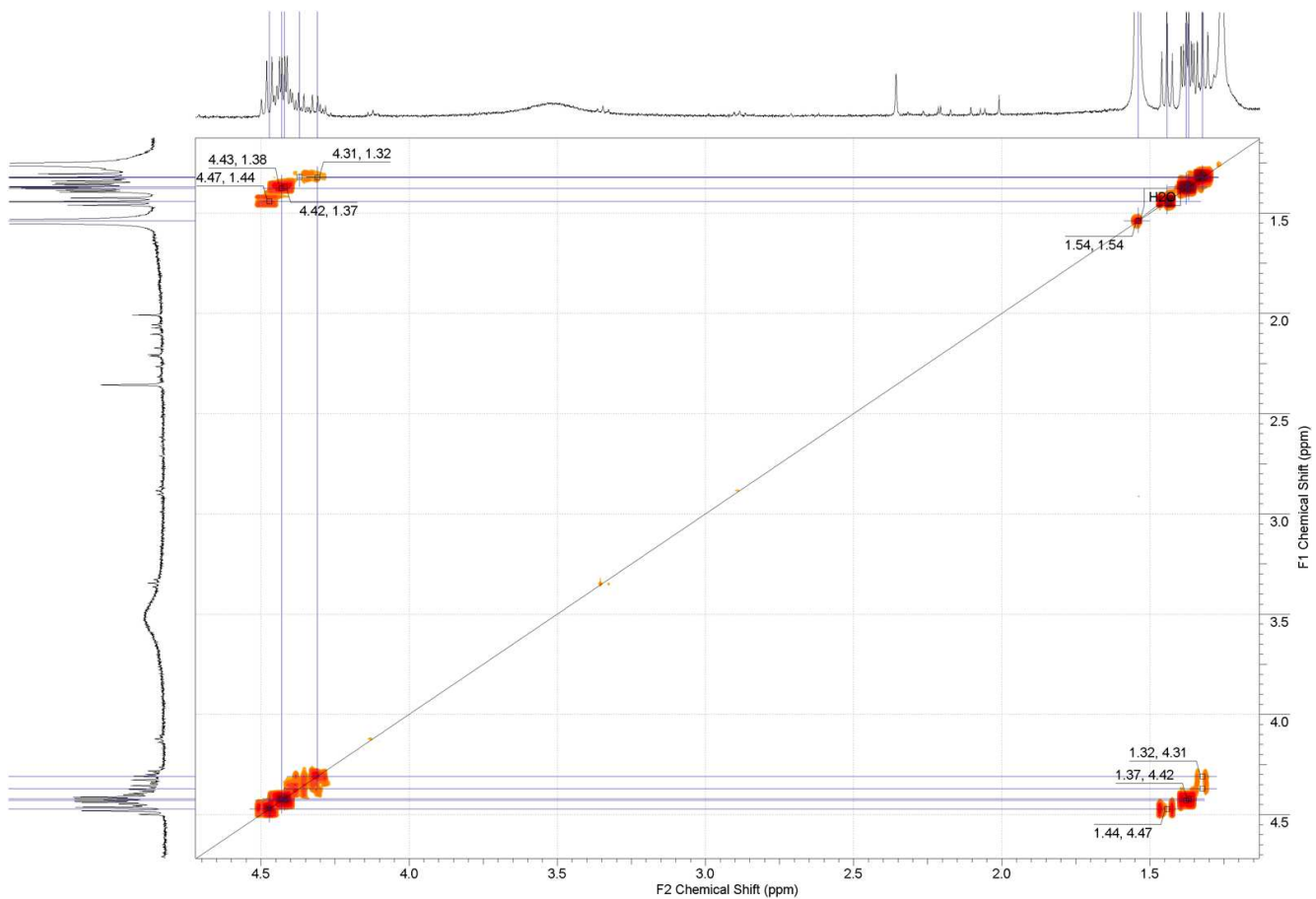


Figure S18. 2D COSY ^1H NMR spectrum of $\text{C}_{70}(\text{CF}_3)_8[\text{C}(\text{CO}_2\text{Et})_2]_2$

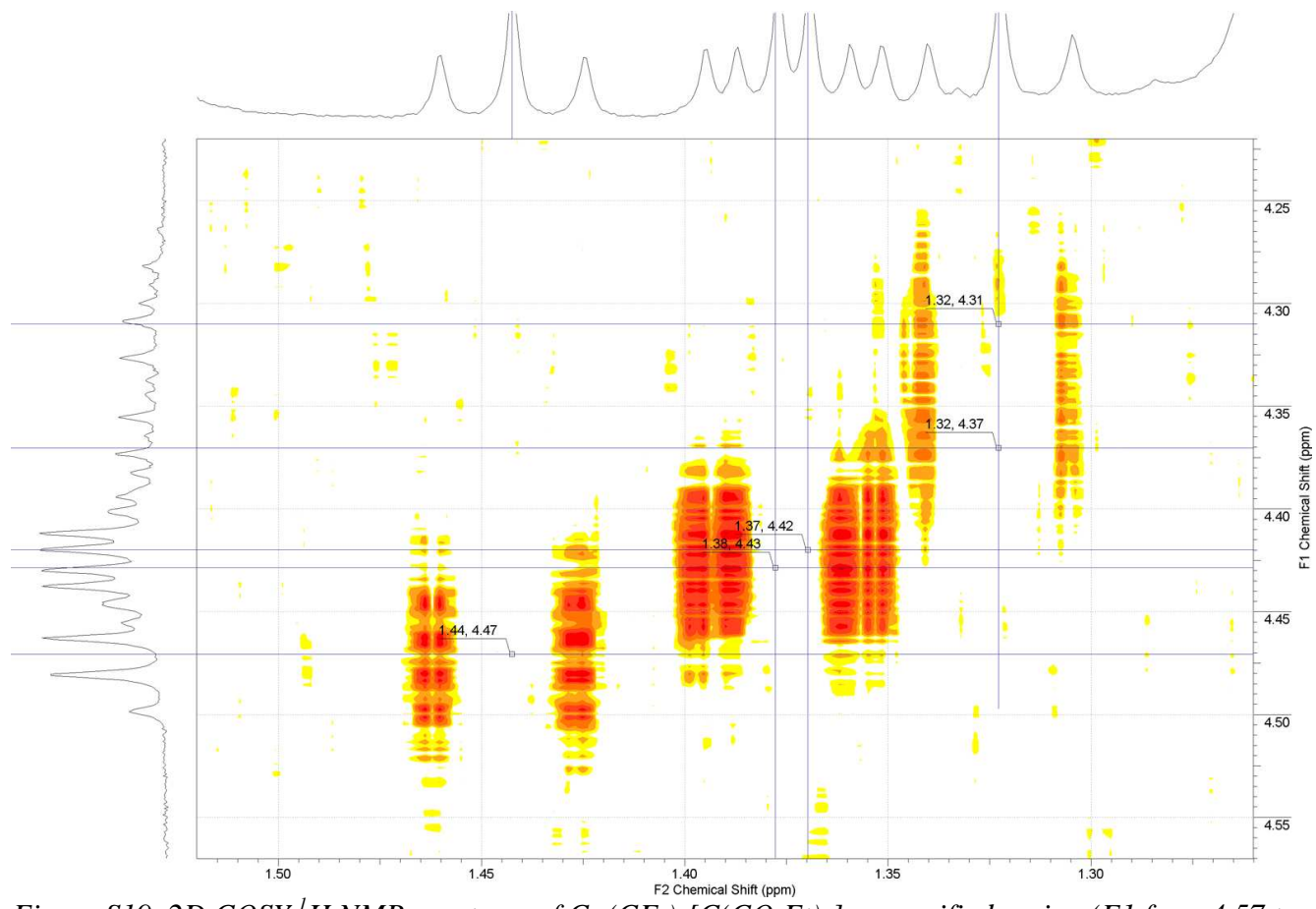


Figure S19. 2D COSY ^1H NMR spectrum of $\text{C}_{70}(\text{CF}_3)_8[\text{C}(\text{CO}_2\text{Et})_2]_2$, magnified region (F1 from 4.57 to 4.22 ppm \times F2 from 1.55 to 1.35 ppm) of Fig.S18.

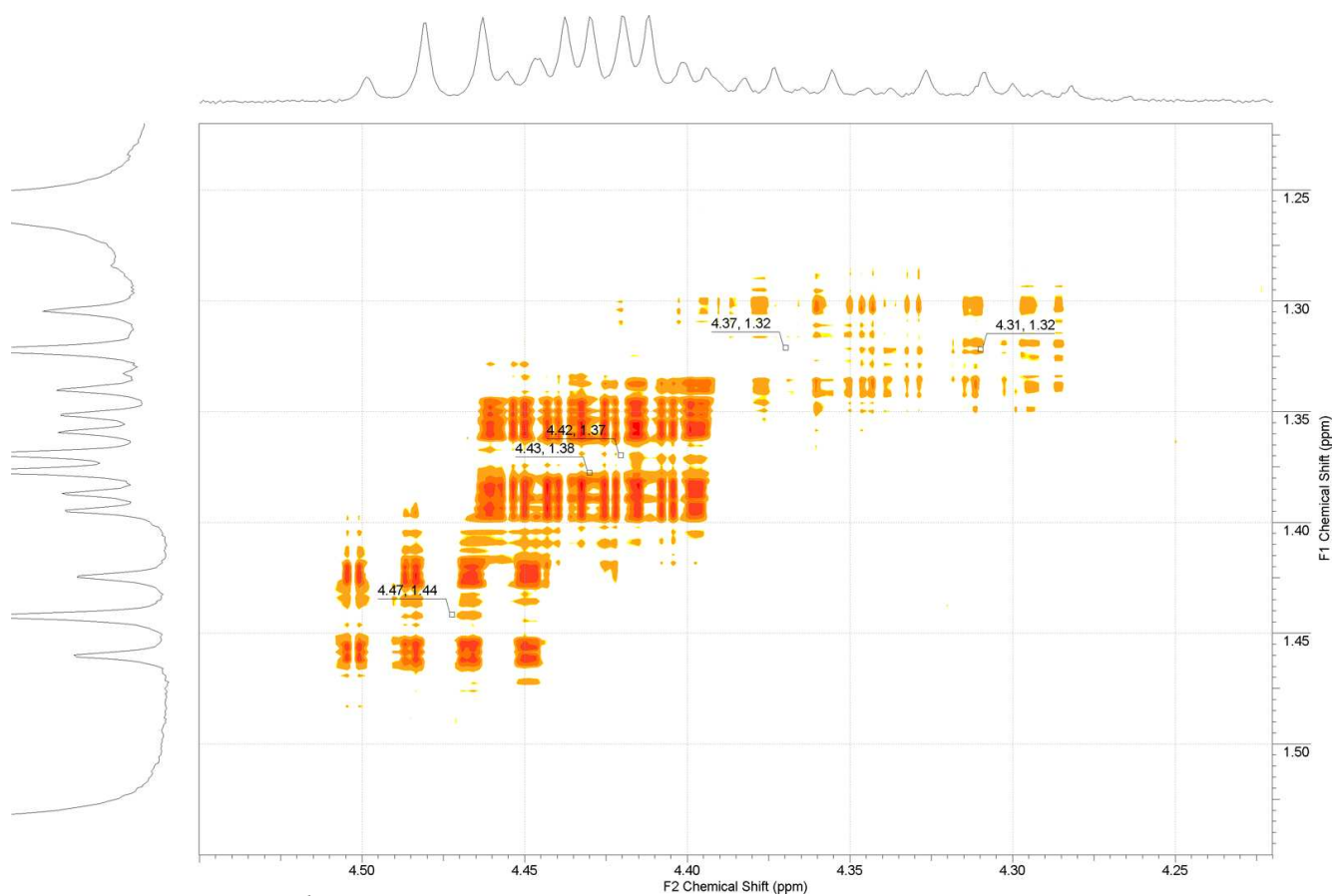


Figure S20. 2D COSY ^1H NMR spectrum of $\text{C}_{70}(\text{CF}_3)_8[\text{C}(\text{CO}_2\text{Et})_2]_2$, magnified region (F1 from 1.55 to 1.22 ppm \times F2 from 4.65 to 4.21 ppm) of Fig.S18.

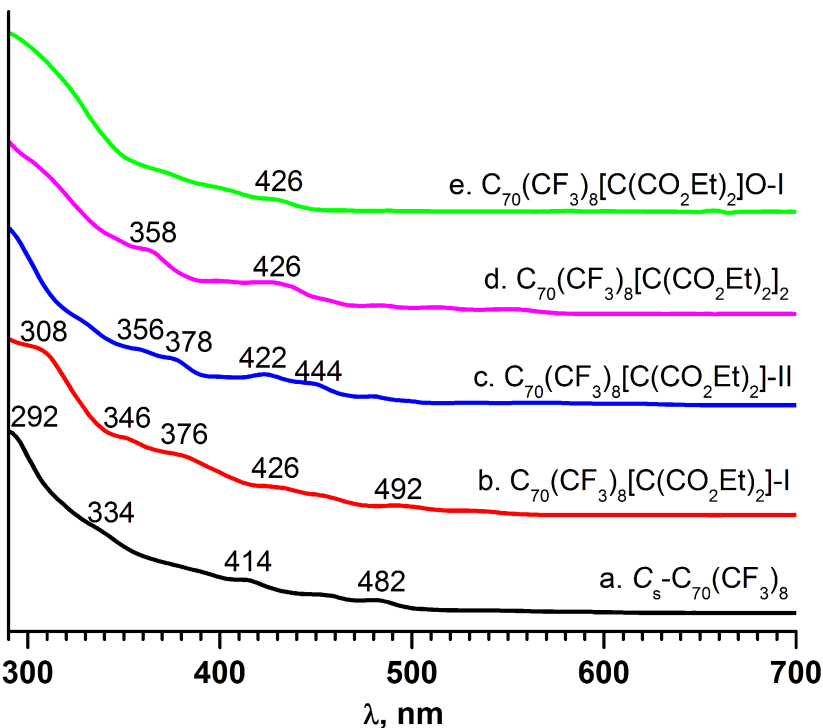


Figure S21. UV/Vis spectra of $C_{70}(CF_3)_8[C(CO_2Et)_2]_n$, $n=1,2$ and $C_{70}(CF_3)_8[C(CO_2Et)_2]O-I$ (290–700 nm, toluene)

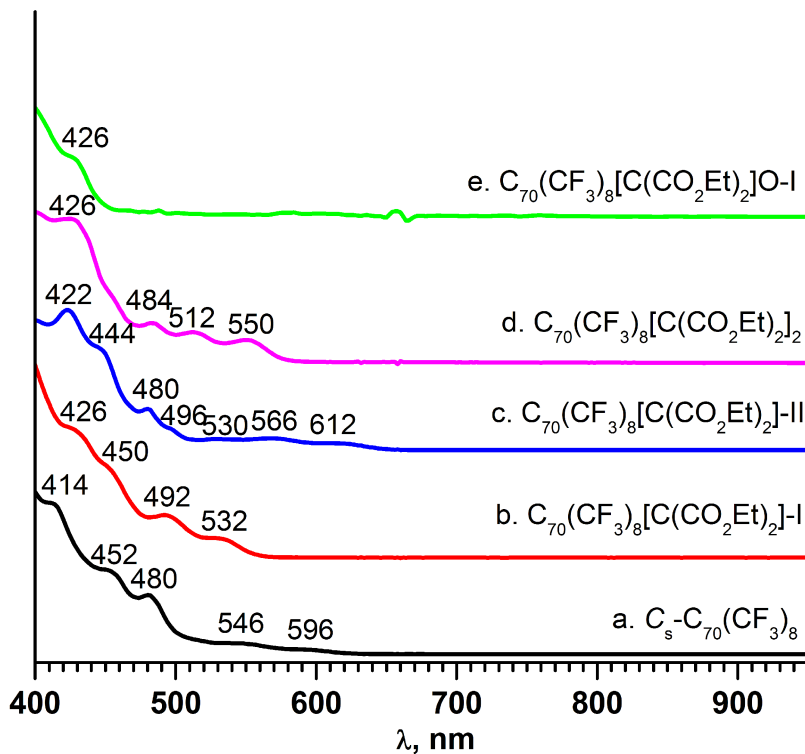


Figure S22. UV/Vis spectra of $C_{70}(CF_3)_8[C(CO_2Et)_2]_n$, $n=1,2$ and $C_{70}(CF_3)_8[C(CO_2Et)_2]O-I$ (400–950 nm, toluene)

Isomer list

The full lists of considered in the work diethyl malonate $C_s\text{-}C_{70}(\text{CF}_3)_8$ mono- and bisadducts include all possible cycloaddition at pairs of adjacent sp^2 cage carbon atoms of $C_s\text{-}C_{70}(\text{CF}_3)_8$ molecule. Also possible $\text{C}_{70}(\text{CF}_3)_8[\text{CBr}(\text{CO}_2\text{Et})_2]^-$ intermediates as well as $\text{C}_{70}(\text{CF}_3)_8\text{H}^-$ anionic species were considered. The total isomers counts, count isomers considered at the AM1, single point DFT (spDFT), and DFT levels of theories are given in the Table S1.

Initially, molecular geometry of the isomers was optimized by TINKER 4.2 molecular mechanic package with MM2 parameter sets [S1]. Further preliminary geometry optimization for these molecules was carried out at the AM1 level of theory with the use of the Firefly QC software (7.1.C,[S2] partially based on GAMESS (US) source code[S3]). Single point DFT calculation of AM1 optimized geometries, final optimizations and calculation of ^{19}F NMR shielding tensors at the DFT level of theory were performed with the use of the PRIRODA v. 6 software.[S4] PBE exchange-correlation functional[S5] and an original basis set of triple zeta quality with (11s6p2d)/[6s3p2d] contraction scheme for second row atoms were used. Calculation of ^{19}F NMR shielding tensors (GIAO method[S6]) of all species involved was carried out for optimized geometries (10^{-5} Hartree/Å RMS energy gradient).

Table S1. Calculation details

$\text{C}_{70}(\text{CF}_3)_8\text{R}_n$		Isomer Count			
R	$n =$	Total	AM1 considered	spDFT	DFT considered
$\text{C}[\text{CO}_2\text{Et}]_2$	1	45	45	45	17 ^b
	2	1585	1585	214 ^a	25 ^c
$\text{CBr}(\text{CO}_2\text{Et})_2^-$	1	33	33	12 ^d	12
H^-	1	33	33	17 ^d	-

^a 100 kJ mol⁻¹ AM1 energy gap; ^b 50 kJ mol⁻¹ spDFT energy gap; ^c 30 kJ mol⁻¹ spDFT energy gap; ^d 50 kJ mol⁻¹ AM1 energy gap;

[S1] TINKER molecular modeling software version 4.2, <http://dasher.wustl.edu/tinker/index.html>

[S2] A. A. Granovsky, Firefly version 7.1.C, <http://classic.chem.msu.su/gran/firefly/index.html>

[S3] M. W. Schmidt, K. K. Baldridge, J. A. Boatz, S. T., Elbert,M. S. Gordon, J. J. Jensen, S. Koseki, N. Matsunaga, K. A., Nguyen, S. Su, T. L.Windus, M. Dupuis and J. A. Montgomery, *J. Comput. Chem.*, 1993, 14, 1347.

[S4] D. N. Laikov, *Chem. Phys. Lett.*, 1997, **281**, 151.

[S5] J. P. Perdew, K. Burke, M. Ernzerhof, *Phys. Rev. Lett.*, 1996, **77**, 38656.

[S6] J. R. Cheeseman, G. W. Trucks, T. A. Keith and M. J. Frisch. *J. Chem. Phys.*, 1996, 104, 5497.

Table S2. Schlegel diagrams, relative energies (at the DFT, single point DFT and AM1 levels of theory) for the most stable isomers of $C_{70}(CF_3)_8C(CO_2Et)_2$ within the DFT energy gap of 40 kJ mol⁻¹. Experimental observed isomers are marked by gray filling.

#	$C_{70}(CF_3)_8[C(CO_2Et)_2]$ Schlegel diagram	$\Delta E, \text{kJ}\cdot\text{mol}^{-1}$			#	$C_{70}(CF_3)_8[C(CO_2Et)_2]$ Schlegel diagram	$\Delta E, \text{kJ}\cdot\text{mol}^{-1}$		
		DFT	spDFT	AM1			DFT	spDFT	AM1
1		0.0	0.0	0.0	6		23.7	26.1	13.0
2		12.3	15.2	-1.8	7		26.0	30.6	13.5
3		16.5	17.5	10.1	8		27.5	27.6	-9.4
4		19.4	17.4	5.5	9		27.9	30.6	-0.2
5		23.5	25.4	14.1	10		31.8	29.4	-13.2

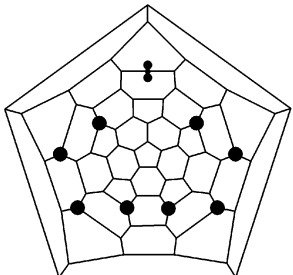
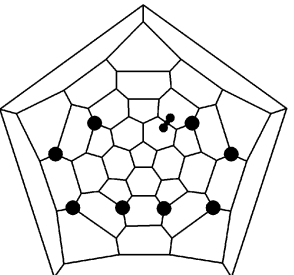
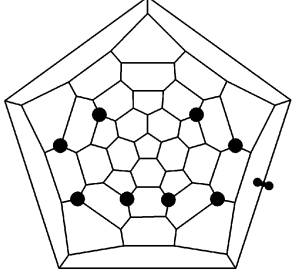
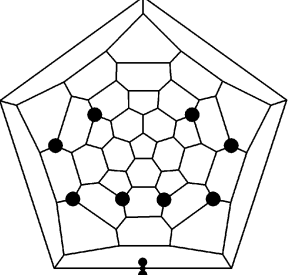
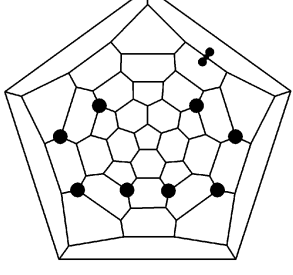
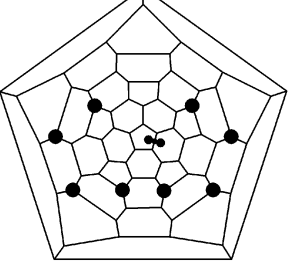
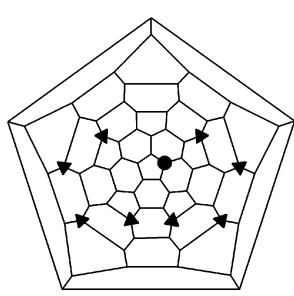
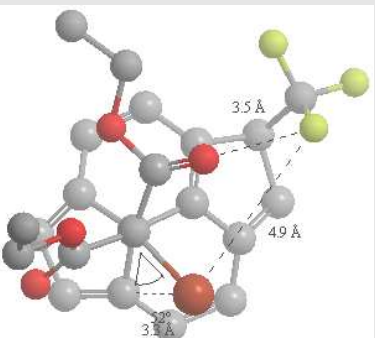
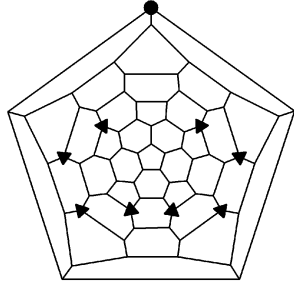
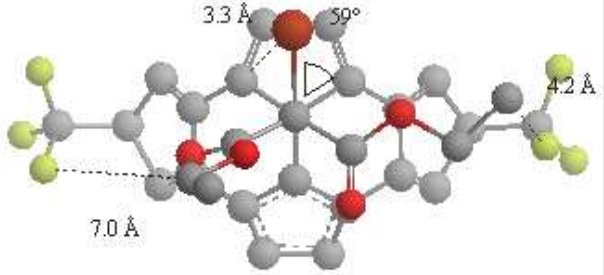
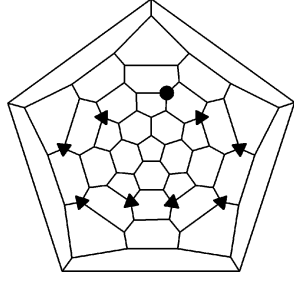
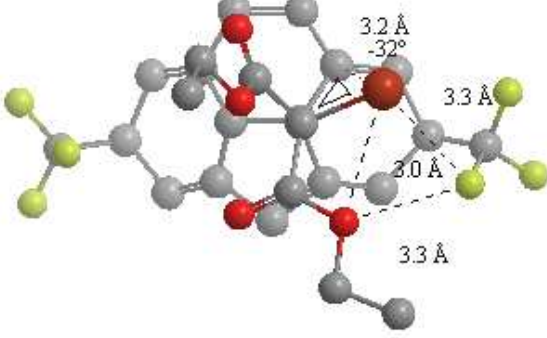
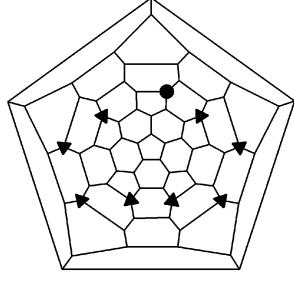
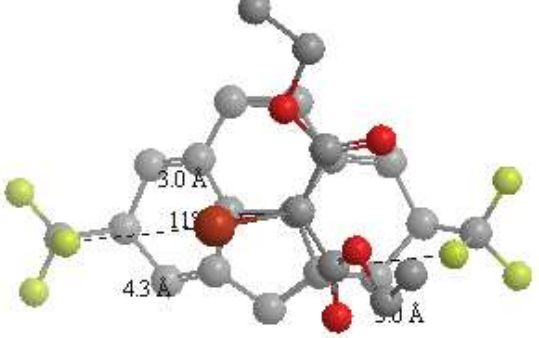
#	$C_{70}(CF_3)_8[C(CO_2Et)_2]$ Schlegel diagram	$\Delta E, \text{kJ}\cdot\text{mol}^{-1}$			#	$C_{70}(CF_3)_8[C(CO_2Et)_2]$ Schlegel diagram	$\Delta E, \text{kJ}\cdot\text{mol}^{-1}$		
		DFT	spDFT	AM1			DFT	spDFT	AM1
11		32.7	36.4	-9.7	14		35.5	34.7	39.6
12		32.8	36.4	4.2	15		36.5	34.9	-10.9
13		32.9	43.5	29.5	16		36.8	36.7	-8.5

Table S3. Schlegel diagrams, relative energies (at the DFT, single point DFT and AM1 levels of theory) for the most stable anions $C_{70}(CF_3)_8CBr(CO_2Et)_2^-$ within the DFT energy gap of 50 kJ mol⁻¹. The corresponding energy values of $C_{70}(CF_3)_8H^-$ with same addend moiety are given in the brackets. Intermediates leading to experimental observed isomers are marked by gray filling.

#	$C_{70}(CF_3)_8[CBr(CO_2Et)_2]^-$ Schlegel diagram	$\Delta E, \text{kJ}\cdot\text{mol}^{-1}$			#	$C_{70}(CF_3)_8[CBr(CO_2Et)_2]^-$ Schlegel diagram	$\Delta E, \text{kJ}\cdot\text{mol}^{-1}$		
		DFT	spDFT	AM1			DFT	spDFT	AM1
1		0.0	0.0 (0.0)	0.0	5		23.4	31.4 (31.8)	30.7
2		7.4	16.2 (18.9)	10.0	6		27.2	37.7 (46.4)	26.1
3		18.4- 22.8	29.3 (-9.4)	14.7- 27.1	7		29.9	43.5 (44.4)	29.1
4		18.6	15.6 (24.5)	10.5	8		32.7	42.2 (43.4)	31.6

#	$C_{70}(CF_3)_8[CBr(CO_2Et)_2]^-$ Schlegel diagram	$\Delta E, \text{ kJ}\cdot\text{mol}^{-1}$			#	$C_{70}(CF_3)_8[CBr(CO_2Et)_2]^-$ Schlegel diagram	$\Delta E, \text{ kJ}\cdot\text{mol}^{-1}$		
		DFT	spDFT	AM1			DFT	spDFT	AM1
9		33.4	44.6 (36.4)	37.1	11		43.4	45.9	43.2
10		34.6	43.4	37.9					

Table S4: Schlegel diagrams, relative DFT energies and fragments of 3D projections of $C_{70}(CF_3)_8[CBr(CO_2Et)_2]^-$ anionic intermediates. Intermediates leading to experimental observed isomers are marked by gray filling.

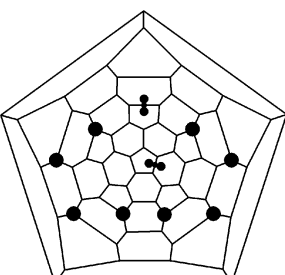
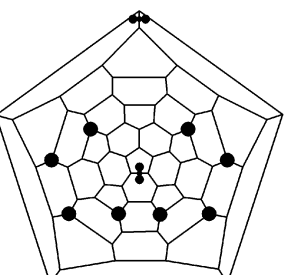
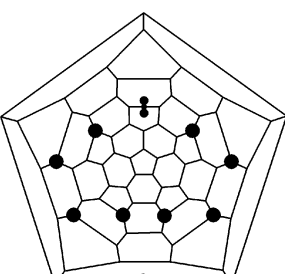
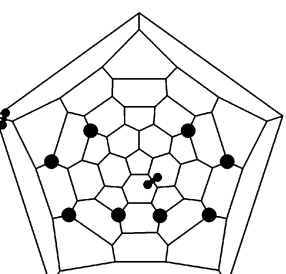
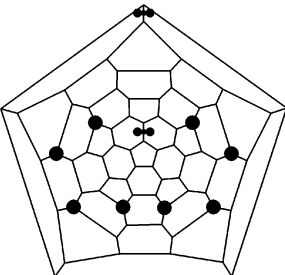
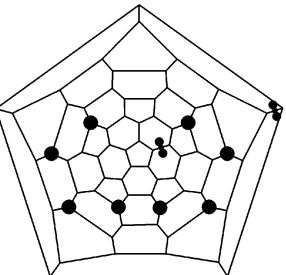
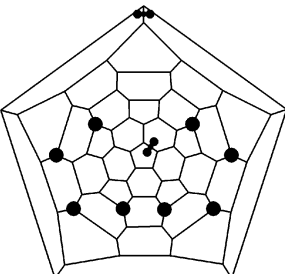
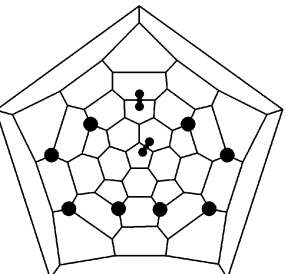
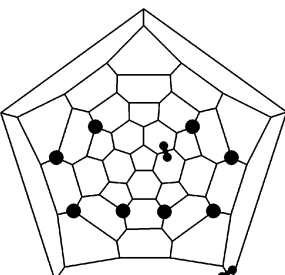
#	$C_{70}(CF_3)_8[CBr(CO_2Et)_2]^-$ Schlegel diagram	DFT $\Delta E, \text{kJ}\cdot\text{mol}^{-1}$		3D projections of intermediate
		Intermediate	Product	
1		0.0	19.4	
2		7.4	12.3	
3		18.4	0.0	
4		22.8	0.0	

5		29.9	16.2

6		34.6	25.5

Table S5. Schlegel diagrams, relative energies (at the DFT, single point DFT and AM1 levels of theory) for the most stable isomers of $C_{70}(CF_3)_8[C(CO_2Et)_2]_2$ within the DFT energy gap of 30 kJ mol⁻¹. Experimental observed isomer is marked by gray filling.

#	$C_{70}(CF_3)_8[C(CO_2Et)_2]_2$ Schlegel diagram	$\Delta E, \text{kJ}\cdot\text{mol}^{-1}$			#	$C_{70}(CF_3)_8[C(CO_2Et)_2]_2$ Schlegel diagram	$\Delta E, \text{kJ}\cdot\text{mol}^{-1}$		
		DFT	spDFT	AM1			DFT	spDFT	AM1
1		0.0	0.0	0.0	6		17.2	20.4	4.0
2		7.0	3.7	14.7	7		18.4	14.6	12.3
3		8.7	5.3	15.3	8		18.8	14.4	-9.4
4		13.0	10.8	14.5	9		19.7	20.0	8.2
5		14.2	12.2	17.8	10		19.9	14.8	7.8

#	$C_{70}(CF_3)_8[C(CO_2Et)_2]_2$ Schlegel diagram	$\Delta E, \text{kJ}\cdot\text{mol}^{-1}$			#	$C_{70}(CF_3)_8[C(CO_2Et)_2]_2$ Schlegel diagram	$\Delta E, \text{kJ}\cdot\text{mol}^{-1}$		
		DFT	spDFT	AM1			DFT	spDFT	AM1
11		23.4	20.2	-6.8	16		28.1	29.5	1.8
12		25.1	22.3	-6.0	17		28.4	26.6	28.9
13		26.3	28.8	15.6	18		28.8	30.2	23.6
14		27.3	27.3	-7.4	19		29.2	27.7	10.3
15		27.3	21.5	19.9					